



U-Net-based flood segmentation using sentinel-1 SAR imagery in Zimbabwe

Tambirai Gahadza, Prof. Achmad Wajdi Farid, Simbarashe Mugova

¹Indonesia Defense University, School of Science and Technology, Kawasan IPSC Sentul, Jl. Anyar, Sukahati, Kec. Citeureup, Kabupaten Bogor, Jawa Barat 16810, Indonesia

DOI: <https://doi.org/10.51244/IJRSI.2026.130600001>

Received: 14 May 2026; Accepted: 19 May 2026; Published: 16 June 2026

ABSTRACT

Flooding is a devastating climate-induced hazard that has severe effects in Sub-Saharan Africa, resulting in significant human, economic, environmental, and losses. Climatic changes have increased the frequency of flood events in Zimbabwe, especially in regions with high rainfall, such as Chimanimani. This investigation introduces a semantic segmentation framework for the detection of flooding that is based on U-Net and employing Sentinel-1 Synthetic Aperture Radar (SAR) imagery. The proposed model enhances flood mapping under cloud-cover conditions through the use of all-weather and day-night imaging capabilities of SAR. Preprocessing procedures which were implemented to enhance model generalization and mitigate class imbalance include speckle noise reduction, image normalization as well as binary mask generation. The model was evaluated and trained using benchmark flood datasets that included Sentinel-1 SAR imagery. The experimental results showed that the segmentation performance was exceptionally good, with an overall precision of 95%, F1-score of 0.88 and recall of 0.82 for flooded regions. Further, the intersection over Union (IoU) analysis confirmed the accurate delineation of floods at pixel level. The results prove the practicality of convolutional neural network-based SAR flood segmentation techniques for real-time disaster monitoring in Zimbabwe and provide a reliable and flexible system for future implementation with real-time meteorological data as well as national early warning mechanisms.

Keywords: Flood Segmentation, U-Net, Sentinel-1 SAR, Deep Learning, Semantic Segmentation,

INTRODUCTION

Background

Flooding is a disturbing natural disaster on a global scale, which has resulted in substantial economic, environmental, and humanitarian losses year by year (Ntajal et al., 2017; Rathupetsane & Kganyago, 2026). The scale of flood events have been exacerbated, particularly in developing countries by climate variability, and other bad environmental practices (Ray et al., 2022). Over the past two decades, floods have impacted billions of individuals worldwide and continue to pose serious threats to agriculture, infrastructure, and human security, according to the World Meteorological Organization (Dube et al., 2018; Sharma et al., 2020). The impacts of extreme hydrological events are further worsened in low-income countries by lack of emergency preparation systems and flood monitoring infrastructure (Ray et al., 2022).

Despite Sub-Saharan Africa minimal contribution to global greenhouse gas emissions, it is becoming more vulnerable to climate-induced disasters. Emergency response systems are being strained by recurring flood disasters in countries such as Mozambique, Nigeria, Sudan, and Zimbabwe (Dube et al., 2018; Rathupetsane & Kganyago, 2026). In recent years flooding has emerged as a perennial environmental challenge in Zimbabwe as a result of cyclonic systems emerging from the Indian Ocean which result in extreme rainfall events. The country's susceptibility to hydrometeorological disasters was witnessed by the catastrophic consequences of Cyclone Idai, which hit the Zimbabwe in 2019 and resulted in considerable deaths, and severe infrastructural



destruction, with Chimanimani and Chipinge districts being the most affected (Rathupetsane & Kganyago, 2026).

In Zimbabwe, conventional flood monitoring methods heavily rely on weather reports and delayed field reporting (Chanza et al., 2020). Institutions such as the Civil Protection Unit and Meteorological Services Department do have existing systems that are limited by technological capacity, lack of coverage, and prolonged dissemination of disaster information (Munsaka et al., 2021; Williamson et al., 2023). The effectiveness of emergency response operations is reduced by these constraints, which brings about the need of a scalable, automatic, and near-real-time flood detection model (Sharma et al., 2020).

Recently, environmental monitoring capabilities have been enhanced by developments in artificial intelligence and remote sensing. SAR imagery has become a viable alternative for flood detection due to its ability to function in all weather conditions (Das et al., 2025; Edwing et al., 2025). In contrast to optical imagery, SAR sensors are capable of acquiring high-resolution surface information during severe weather conditions through the penetration of cloud cover (Huang et al., 2024; Wu et al., 2019). The Sentinel-1 mission of the European Space Agency offers C-band SAR imagery that is readily available to continuously feed flood detection applications (Munawar et al., 2021; Thapa et al., 2022).

Deep learning techniques, including CNNs, are effective for semantic segmentation and satellite image analysis (Pech-May et al., 2024). Architectures such as U-Net, SegNet, and DeepLabv3+ which are capable of learning intricate spatial features from remotely sensed imagery has enabled them to achieve high segmentation accuracy in flood mapping applications (Pech-May et al., 2024; Zhao et al., 2022). However, the majority of current research have been conducted outside of Africa, which restricts the applicability of these methods to Zimbabwean environments that exhibit significant differences in vegetation, and climate conditions.

Building on these findings, this research proposes a powerful semantic segmentation framework based on U-Nets to automate flood detection in Zimbabwe using Sentinel-1 SAR imagery. The study explores how effectively a U-Net-based CNN can identify flooded regions in Zimbabwe's unique environment, thereby paving the way for seamless integration with real-time emergency monitoring systems.

Importance of the Problem

Flood monitoring systems are important for reducing disaster impacts and improving emergency response in Zimbabwe, where recurrent flooding continues to affect communities, infrastructure, agriculture, and livelihoods. However, conventional flood monitoring approaches remain constrained by delayed reporting, limited spatial coverage, and the scarcity of real-time observations.

Synthetic Aperture Radar (SAR) images offer a good alternative because they allow monitoring in any weather and at any time, avoiding problems caused by clouds and bad weather that affect regular cameras. When integrated with deep learning methods such as U-Net semantic segmentation, SAR data can support automated and accurate flood extent mapping.

Despite recent progress in SAR-based flood detection, most studies have focused on Europe, Asia, and North America, with limited adaptation to Sub-Saharan African environments where data scarcity and limited validation resources remain major challenges. Consequently, this study evaluates a U-Net framework using Sentinel-1 SAR imagery to improve flood detection capability under Zimbabwean conditions and support disaster risk management applications

LITERATURE REVIEW

Research in flood detection has been substantially improved following recent strides in artificial intelligence and remote sensing. The widespread adoption of SAR imagery in flood surveillance is due to its capacity to capture surface information in extreme weather conditions (Amit & Aoki, 2017; Homepage et al., 2022). Raspini et al.,



2018 conducted research that illustrated the efficacy of Sentinel-1 SAR imagery in flood mapping during catastrophic weather events, where optical imagery was rendered unreliable by cloud obstruction.

The accuracy of flood detection tasks has been extensively enhanced by the incorporation of deep learning approaches (Miau & Hung, 2020a; Stateczny et al., 2023). Semantic segmentation approaches that make use of CNNs, including DeepLabv3+, SegNet, and U-Net, are frequently employed due to their ability to acquire structured spatial depictions from satellite imagery (Edwing et al., 2025; Miau & Hung, 2020b). U-Net was first created for biomedical image segmentation. It uses an encoder-decoder structure with skip connections to keep spatial details during segmentation (Pech-May et al., 2024; Zhao et al., 2022). This architecture has been effectively adapted for remote sensing applications.

A number of studies have reported robust segmentation performance when Sentinel-1 SAR imagery is combined with CNN-based architectures (Moghimi et al., 2024; Pally & Samadi, 2022). Recent researches have illustrated that semantic segmentation techniques can be employed to obtain high flood detection accuracy in deep learning-based SAR segmentation approaches (Rathupetsane & Kganyago, 2026). In the same vein, Windheuser investigated multimodal deep learning frameworks that integrated SAR imagery with weather and hydrological datasets to enhance the predictive capabilities of flood monitoring (Windheuser et al., 2023).

While these studies shown encouraging outcomes, the majority of the current studies utilized datasets gathered from Asia, Europe, or North America (Ntajal et al., 2017). African flood-prone regions are relatively underrepresented in the research on deep learning-based flood detection (Umar & Gray, 2023). As a result, models built using data from outside Africa may not work as well when applied in Zimbabwe.

Moreover, prior research predominantly focused on overall flood mapping efficacy rather than its eventual integration within disaster management frameworks (Pascaline et al., 2018; Ray et al., 2022). In Zimbabwe, flood monitoring systems are hindered by tardy reporting protocols and inadequate technology infrastructure (Rathupetsane & Kganyago, 2026). This study thus expands upon prior research by modifying deep learning-based SAR flood segmentation methods for flood-prone regions in Zimbabwe, while highlighting its practical importance for disaster monitoring.

Hypotheses and Study Contribution

This study investigates whether a U-Net-based semantic segmentation framework can effectively detect flooded areas using Sentinel-1 SAR imagery under Zimbabwean environmental conditions. The central hypothesis states that the proposed U-Net framework can achieve high flood detection accuracy through SAR-based semantic segmentation.

The study is grounded in deep learning semantic segmentation theory, particularly encoder-decoder CNN architectures for pixel-level image classification. The framework aims to support scalable flood monitoring and disaster management applications in Zimbabwe and similar flood-prone regions.

This study makes several key contributions:

1. Development of a U-Net-based semantic segmentation framework for flood detection using Sentinel-1 SAR imagery.
2. Evaluation of pixel-level flood segmentation performance using standard semantic segmentation metrics.
3. Adaptation of SAR-based flood mapping techniques to Zimbabwean environmental conditions.
4. Provision of a scalable framework for future integration with meteorological and disaster management systems

METHODOLOGY

Research Design

A quantitative experimental research design was employed to develop and evaluate a U-Net-based semantic segmentation framework for automated flood detection and monitoring using Sentinel-1 SAR imagery. The study adopted a supervised deep learning approach in which labeled SAR images and corresponding flood masks were used to train the model for pixel-level classification of flooded and non-flooded regions.

The research workflow comprised dataset acquisition, preprocessing, U-Net implementation, model training, and performance evaluation. The dataset was split into training, validation, and test sets to prevent data leakage and ensure unbiased evaluation. Model performance was evaluated using Intersection over Union (IoU), Dice coefficient, precision, recall, and F1-score.

Dataset Acquisition

The study utilized Sentinel-1 SAR imagery and corresponding binary flood masks obtained from publicly available benchmark flood datasets and Kaggle repositories. Sentinel-1 imagery was selected because SAR sensors operate independently of weather and light conditions, making them suitable for flood monitoring during extreme rainfall events. The dataset comprised paired SAR pictures and labeled segmentation masks indicating flooded and non-flooded areas. Duplicate samples and corrupted instances were omitted to enhance dataset consistency. The chosen final picture showed flood-prone conditions, including river and vegetated landscapes. The dataset was split into training (70%), validation (15%), and test (15%) sets. The training set helped the model learn, the validation set was used to check settings, and the testing set measured the final performance.

Data Preprocessing

Data preprocessing was conducted to promote consistency, diminish variability in SAR images, and facilitate model convergence. The preprocessing pipeline comprised image normalization, scaling, binary mask generation, and data augmentation.

Image Normalization and Resizing

All SAR images were standardized to mitigate intensity fluctuations and enhance the numerical reliability during training. Images and their respective segmentation masks were scaled to consistent spatial dimensions suitable for the U-Net architecture. Binary masks were created to designate flooded areas as foreground pixels and non-flooded areas as background pixels.

Data Augmentation

Data augmentation was used to help the model generalize better and reduce overfitting. The augmentation procedure comprised horizontal and vertical rotation, zooming, and movement operations. These modifications enhanced spatial variety while maintaining the characteristics of flood regions.

U-Net Architecture

The suggested system utilized a U-Net CNN model for semantic segmentation. U-Net was chosen for its efficiency in pixel-level segmentation and its ability to maintain intricate spatial details via encoder-decoder architecture and skip connections. Figure 1 below presents the model architecture for U-Net model:

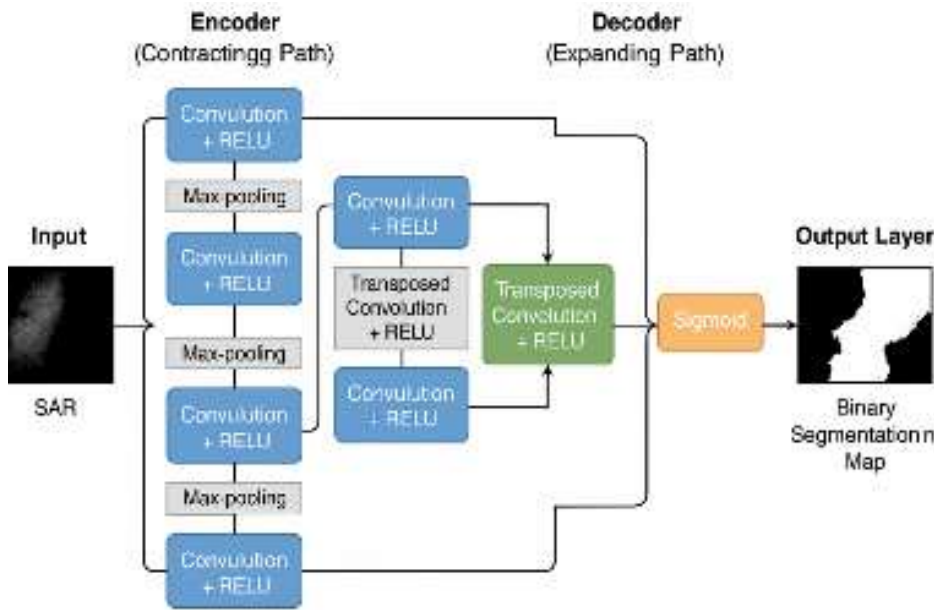


Figure 1: Model Architecture

The architecture was composed of a decoder network for spatial reconstruction and an encoder network for hierarchical feature extraction. Max-pooling operations, convolutional layers, sigmoid activation, batch normalization, and ReLU activation functions were implemented throughout the network to produce the segmentation map.

Encoder Network

The encoder structure extracted hierarchical spatial characteristics from the SAR picture using iterative convolution and max-pooling operations. The contracting pathway systematically diminished spatial dimensions while acquiring contextual cues related to flooding.

Decoder Network

Segmentation masks were rebuilt by the decoder network using convolution and up sampling techniques. This procedure produced flood forecasts at the pixel level and restored spatial resolution.

Skip Connections

Skip connections carried high-resolution feature maps directly from the encoder layers to their matching decoder layers, preserving crucial details throughout the network. During segmentation, the method enhanced flood-boundary localization while maintaining spatial details.

MODEL TRAINING

Training Configuration

The experiments were conducted using Python with TensorFlow and Keras libraries for implementation of the U-Net semantic segmentation framework. Model training and evaluation were performed in the Kaggle python environment using GPU acceleration to improve computational efficiency. Sentinel-1 SAR imagery together with Sen1Floods11 and SEN12-FLOOD benchmark datasets were used for training and validation. The dataset was divided into training, validation, and testing subsets in a 70:15:15 ratio. During training, mini-batch learning was utilized, and augmented data were dynamically incorporated to enhance generalization. Validation monitoring was employed to mitigate overfitting and evaluate convergence stability.



Loss Function

Binary Cross-Entropy (BCE) loss was utilized during model training to enhance pixel-wise categorization between flood and non-flood areas. The loss function quantifies prediction error by contrasting model outputs with reference flood masks and is extensively utilized in binary semantic segmentation tasks. Its appropriateness for imbalanced target distributions renders it suitable for SAR-based flood mapping applications.

Performance Evaluation

The model's performance was assessed using standard semantic segmentation metrics using novel test data to evaluate flood delineation accuracy and segmentation efficacy.

Intersection Over Union (IoU)

Intersection over Union (IoU) was employed to measure the geographic congruence between anticipated flood areas and reference flood masks. Elevated IoU values signify enhanced concordance and segmentation efficacy.

Dice Coefficient

The Dice coefficient was utilized to assess the similarity between predicted flood masks and ground reference masks. The statistic indicates the uniformity of segmentation and the quality of overlap.

Precision and Recall

Precision and recall were employed to assess classification reliability and flood detection efficacy. Precision quantifies the accuracy of projected flooded pixels, whereas recall indicates the model's capacity to detect genuine flooded areas.

F1-Score

The F1-score served as a balanced performance metric by integrating precision and recall into one measure. It offers a comprehensive evaluation of detection efficacy, especially in scenarios characterized by class imbalance prevalent in flood segmentation tasks.

Dataset Distribution and Partitioning

The integrated dataset, compiled from Sentinel-1 SAR imagery, SEN12-FLOOD, and Sen1Floods11, was divided into training, validation, and testing subsets to facilitate robust training and evaluation of the proposed flood detection framework. The partitioning strategy was aimed to balance model learning, hyperparameter optimization, and unbiased performance evaluation while reducing risks of overfitting.

A 70–15–15 split strategy was implemented, allocating 70% of the dataset to model training, 15% to validation, and 15% to independent testing. Spatial and temporal separation principles were applied during partitioning to reduce overlap between scenes and improve generalization across diverse flood conditions.

The use of benchmark datasets alongside locally relevant Sentinel-1 imagery strengthened model robustness under conditions of limited ground truth data and improved transferability across heterogeneous flood environments. Figure 2 below presents the dataset preparation and modelling workflow illustrating Sentinel-1 SAR acquisition, preprocessing, benchmark dataset integration, augmentation, partitioning, model training, and flood map generation.

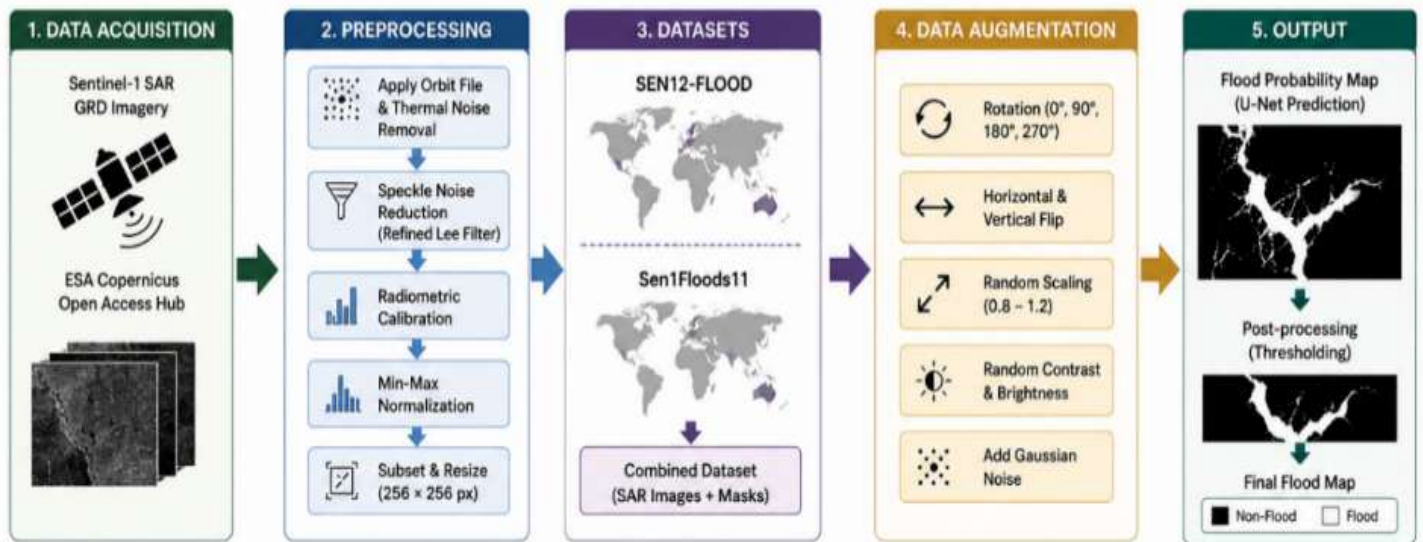


Figure 2. Dataset preparation and modelling workflow illustrating Sentinel-1 SAR acquisition, preprocessing, benchmark dataset integration, augmentation, partitioning, model training, and flood map generation.

Geographic Coverage and Study Area

The study focused on Zimbabwe, a country frequently affected by hydrological disasters including riverine floods, flash floods, and cyclone-induced inundation. Several flood-prone regions were considered to improve representation of different environmental and hydrological settings.

These regions were selected because they represent diverse topographical and climatic conditions while also reflecting areas with recurring flood impacts. The study area included Chimanimani District (Manicaland Province), and selected areas within the Lower Zambezi Basin, representing diverse hydrological and topographical conditions associated with recurrent flooding.

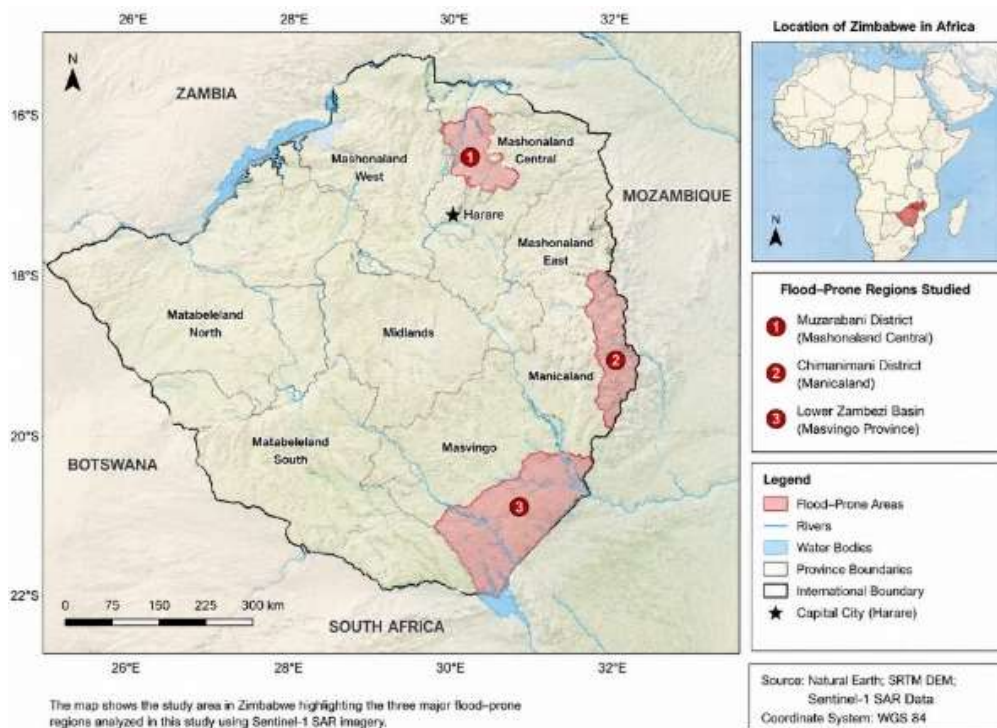


Figure 3: Study area map of flood-prone regions in Zimbabwe



Temporal Coverage

The temporal scope of this study incorporated multi-season flood events and satellite observations to enhance model generalization and minimize temporal bias. Sentinel-1 SAR imagery acquired between 2019 and 2025 was utilized, covering major flood events including the aftermath of Cyclone Idai, seasonal river flooding, and rainfall-induced inundation episodes.

The inclusion of multi-temporal observations enabled the framework to capture diverse flood signatures under varying meteorological and environmental conditions, thereby improving its applicability across different flood scenarios in Zimbabwe.

RESULTS

The experimental results achieved using the suggested U-Net semantic segmentation model for flood detection in Sentinel-1 SAR data are discussed in this section. The classification accuracy, segmentation overlap performance, convergence behavior and visual analysis of the anticipated flood regions also evaluated. Quantitative results are supported by classification metrics, confusion matrix analysis, and pixel-level segmentation evaluation

Segmentation Performance

The classification performance of the proposed model was evaluated using precision, recall, F1-score, and accuracy. The metrics were calculated on previously unexamined testing data to evaluate the framework's efficacy in differentiating between flooded and non-flooded areas. Table 1 displays the classification outcomes derived from the testing dataset.

Table 1. Evaluation metrics for the proposed SAR-based U-Net flood detection framework.

Metric	Value (%)	Description
Accuracy	88.84	Percentage of correctly classified flooded and non-flooded pixels
Precision	95.71	Indicates low false flood detections and reliability of predicted flooded regions
Recall	82.42	Measures the proportion of actual flooded pixels correctly identified
F1-Score	88.57	Harmonic mean of precision and recall showing balanced performance
Intersection over Union (IoU)	79.49	Measures spatial overlap between predicted flood masks and reference labels
Dice Coefficient	88.57	Indicates segmentation quality and preservation of flood boundaries

The framework achieved an overall classification accuracy of 88.84%, demonstrating that most image pixels were accurately classified as either flooded or non-flooded. The precision of 95.71% indicates a low rate of false flood detections and confirms that most predicted flooded areas correspond to actual inundation. The recall rate of 82.42% suggests effective identification of flooded pixels, although certain inundated regions were not detected.

The F1-score reached 88.57%, demonstrating balanced performance between precision and recall. Spatial agreement between predicted masks and reference flood labels was demonstrated by an Intersection over Union (IoU) of 79.49% and a Dice coefficient of 88.57%. These metrics indicate substantial overlap and effective preservation of flood boundaries.

Training and Validation Performance

Accuracy and loss curves generated during training and validation were used to evaluate the model's convergence

behavior. These curves shed light on the model's capacity for generalization, convergence consistency, and learning stability. Figure 4 presents the training and validation results of the U-Net model across all training epochs.

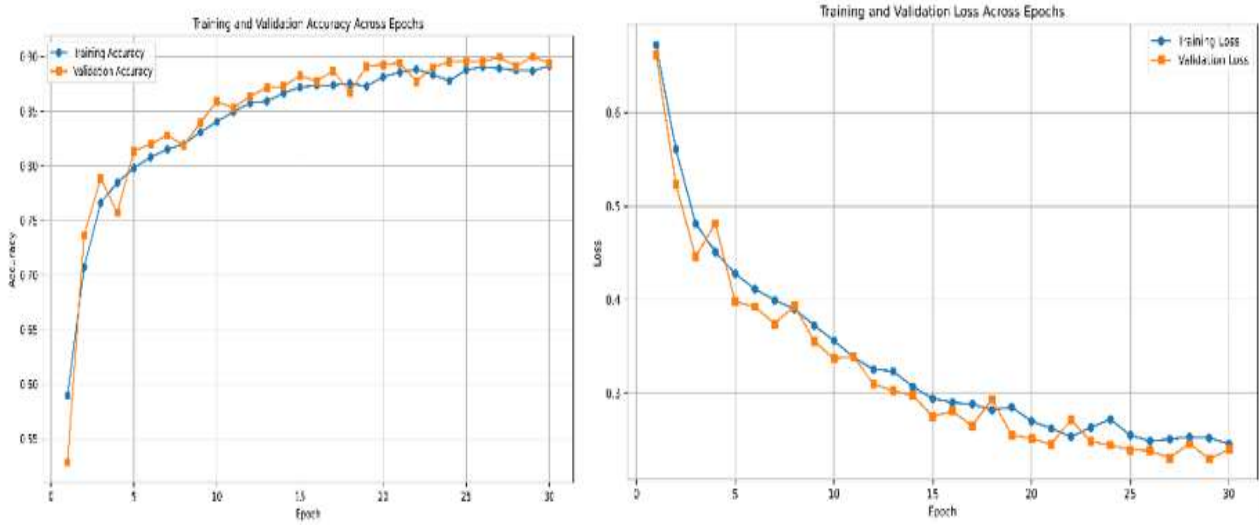


Figure 4: Training and validation performance of the proposed U-Net model across training epochs

The training outcomes exhibited consistent convergence with gradually diminishing loss values over the optimization phase. The validation accuracy was continually elevated with negligible variations, signifying minimal overfitting and robust generalization performance.

Confusion Matrix Analysis

The confusion matrix demonstrated strong classification performance, with most flooded and non-flooded pixels correctly identified. The model produced relatively few false positives, consistent with the high precision value (95.71%). Some false negatives remained visible, corresponding to the recall score (82.42%), indicating that certain inundated regions were not fully detected. This balance between precision and recall is important for operational flood monitoring because minimizing false alarms improves confidence in early warning systems while maintaining effective flood detection capability. Figure 5 presents the confusion matrix obtained from the segmentation experiments.

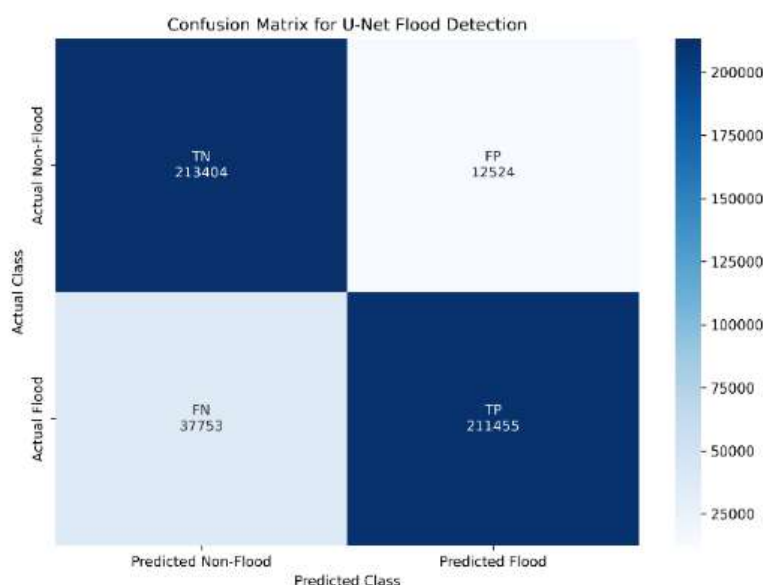


Figure 5: Confusion matrix obtained from the segmentation experiments

The confusion matrix demonstrates that the model effectively differentiates between flooded and non-flooded areas. The majority of samples were accurately identified, with minimal misclassification noted in the testing results.

IoU and Pixel-Level Segmentation Performance

Intersection over union (IoU) and dice coefficient metrics were calculated to evaluate the spatial overlap consistency between predicted segmentation outputs and ground-truth annotations. These metrics are widely used in semantic segmentation as they provide a robust assessment of pixel-level overlap accuracy. The intersection over union and dice coefficient metrics are in figure 6 below:

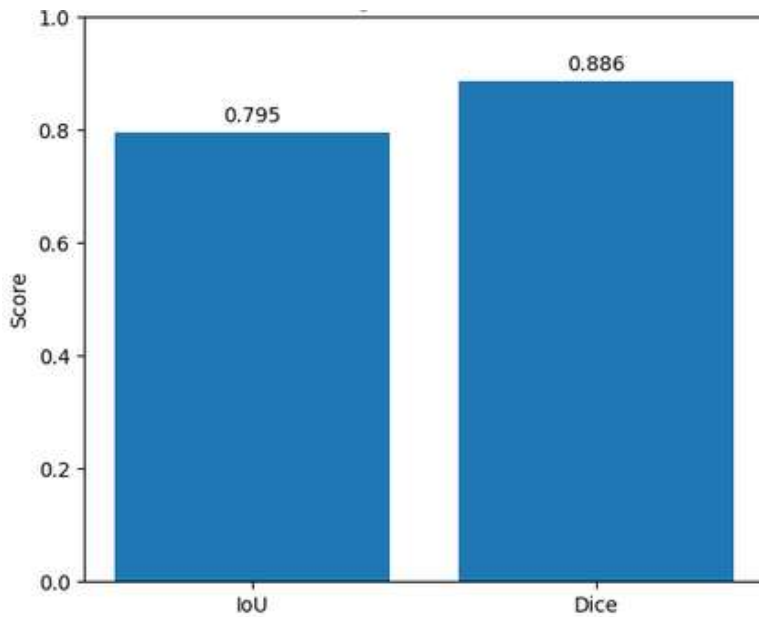


Figure 6: Pixel-Level Segmentation Performance

The IoU and Dice coefficient results demonstrate a strong spatial correspondence between the predicted segmentation masks and the reference flood annotations.

Visual Segmentation Outcomes

Flood Detection Workflow

Figure 7 illustrates the flood detection workflow, showing the progression from raw Sentinel-1 SAR input (left) to the ground-truth flood mask (middle) and the U-Net CNN predicted mask (right).

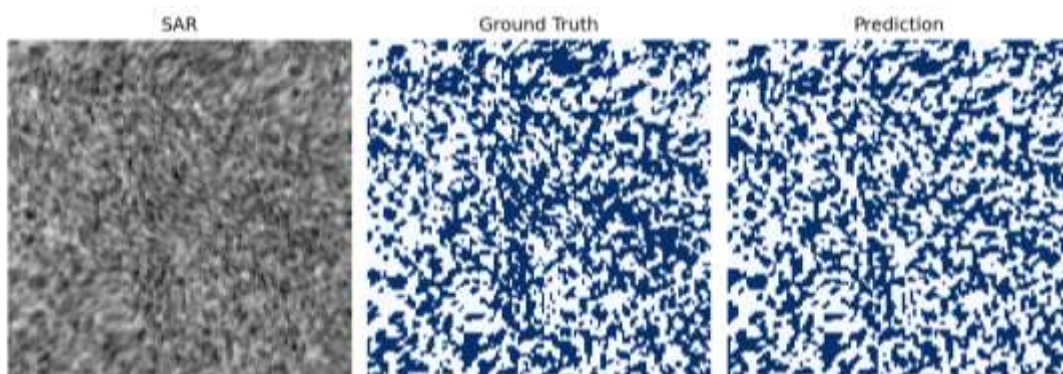


Figure 7: Input SAR, ground truth mask, and predicted mask.

The triplet demonstrates the model’s ability to perform pixel-level flood segmentation. The predicted mask highlights inundated areas with clear spatial precision, validating the segmentation capability of the U-Net and confirming its effectiveness in delineating flooded versus non-flooded regions.

Flood detection on SAR image tiles

Figure 8 displays some examples of flood detection results from different Sentinel 1 SAR tiles, showing the genuine flood state and the model prediction for each. The image illustrates the model’s ability to differentiate between flooded and non-flooded locations at the tile level. Most predictions are very near to ground reality, proving the resilience of U-Net CNN in operational contexts. However, certain false negatives are noticed (e.g., tiles labelled as flooded but predicted as non-flooded), showing both the benefits and limitations of the approach.

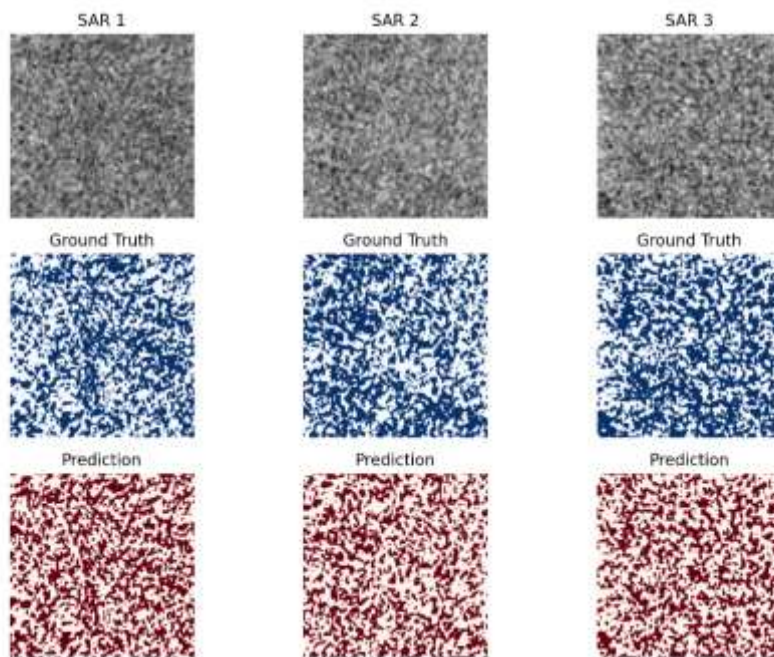


Figure 8. Flood detection results on SAR image tiles.

Visual comparison of before flood vs after flooded

Figure 9 below illustrates the contrast between non-inundated (left) and flooded (right) regions through side-by-side imagery. The comparison demonstrates differences in texture and signal intensity between the two settings.

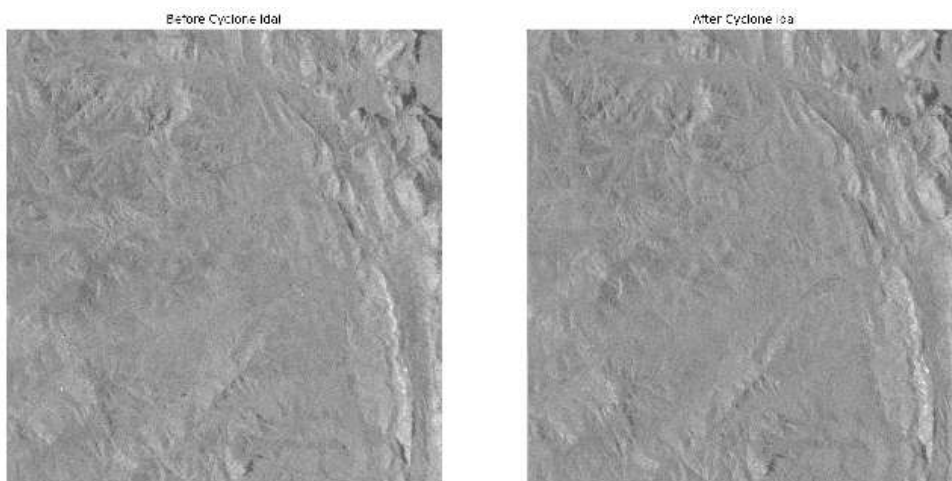


Figure 9: Before flooding and after flooding



These differences illustrate that inundated terrain has different spectral and radar signatures, which makes Sentinel-1 SAR data useful for flood detection and categorization.

DISCUSSION

Effectiveness of SAR-Based CNN Flood Detection

The results indicate that the proposed U-Net framework, when applied to Sentinel-1 SAR imagery, provides reliable flood detection performance in data-limited environments. The model achieved accuracy around 88% with strong precision and recall values, confirming its capability for pixel-level flood segmentation.

These findings reinforce the suitability of SAR imagery for flood monitoring, particularly where optical imagery is constrained by cloud cover and ground observations are limited. The framework successfully delineated both extensive floodplains and smaller fragmented inundation areas, indicating its potential applicability for disaster response and flood monitoring in Zimbabwe.

Strengths of the U-Net Architecture

The encoder–decoder architecture of U-Net effectively captures hierarchical spatial features while preserving fine-scale details through skip connections, contributing to the high segmentation agreement observed through IoU and Dice metrics.

In addition, preprocessing, augmentation, and threshold optimization improved resilience to class imbalance and enhanced detection sensitivity to sparse flood pixels. These characteristics support the suitability of U-Net for SAR-based flood mapping applications in data-limited environments.

Comparative Discussion with Existing Studies

Table 2 presents a comparison between the proposed framework and previous flood detection studies employing benchmark datasets and multimodal approaches.

Table 2: Comparative analysis of flood detection models

Study	Approach	Accuracy	Precision	Recall	IoU / Dice
Bonafilia et al. (2020)	U-Net on Sen1Floods11	≈0.90	0.95	0.88	IoU ≈0.85
Schmitt et al. (2019)	SEN12-FLOOD benchmark	≈0.89	0.93	0.87	Dice ≈0.86
Li et al. (2021)	SAR + meteorological fusion	≈0.92	0.94	0.9	IoU ≈0.87
This study	U-Net + Sentinel-1 SAR	0.888	0.957	0.824	IoU = 0.795; Dice = 0.886

Source: Adapted from Bonafilia et al., Schmitt et al., and Li et al., with results from the present study.

The comparison demonstrates that the proposed framework achieves performance comparable to, and in some instances surpassing, previously reported studies, even under data-constrained conditions. These results indicate that the approach is well-suited for flood monitoring applications in regions with limited annotated datasets

Nevertheless, comparisons should be interpreted cautiously because datasets, environmental conditions, and validation procedures differ across studies. Furthermore, the absence of field validation limits direct comparison with operational flood monitoring systems.

Overall, the findings demonstrate the applicability of the framework for flood monitoring in data-limited regions of Sub-Saharan Africa and support future integration with meteorological, hydrological, and field-based observations.

Field Validation Constraints

Direct field-based validation was not conducted in the current study due to restricted access to flood-affected regions and the absence of synchronized ground observations during flood events in Zimbabwe. The dynamic nature of flooding, together with logistical and temporal constraints, limited direct verification of predicted inundation extents using in-situ observations.

Consequently, validation was performed using benchmark flood datasets, namely **Sen1Floods11** and **SEN12-FLOOD**, which provide standardized flood masks and reference annotations for SAR-based flood segmentation. These benchmark datasets enabled objective evaluation and comparative assessment of model performance under controlled experimental conditions.

In addition, the validation framework considered ancillary information sources, including meteorological observations, hydrological indicators, historical flood records, and expert knowledge where available, to support interpretation of flood extent predictions. The adopted validation workflow is illustrated in Fig. 10.

However, the absence of direct field verification remains a limitation because comparison between predicted flood extents and observed inundation boundaries was not possible. Future work will incorporate field surveys, UAV-based mapping, hydrological measurements, and disaster reports to strengthen validation and improve operational applicability. The adopted validation workflow is illustrated in Fig. 10.

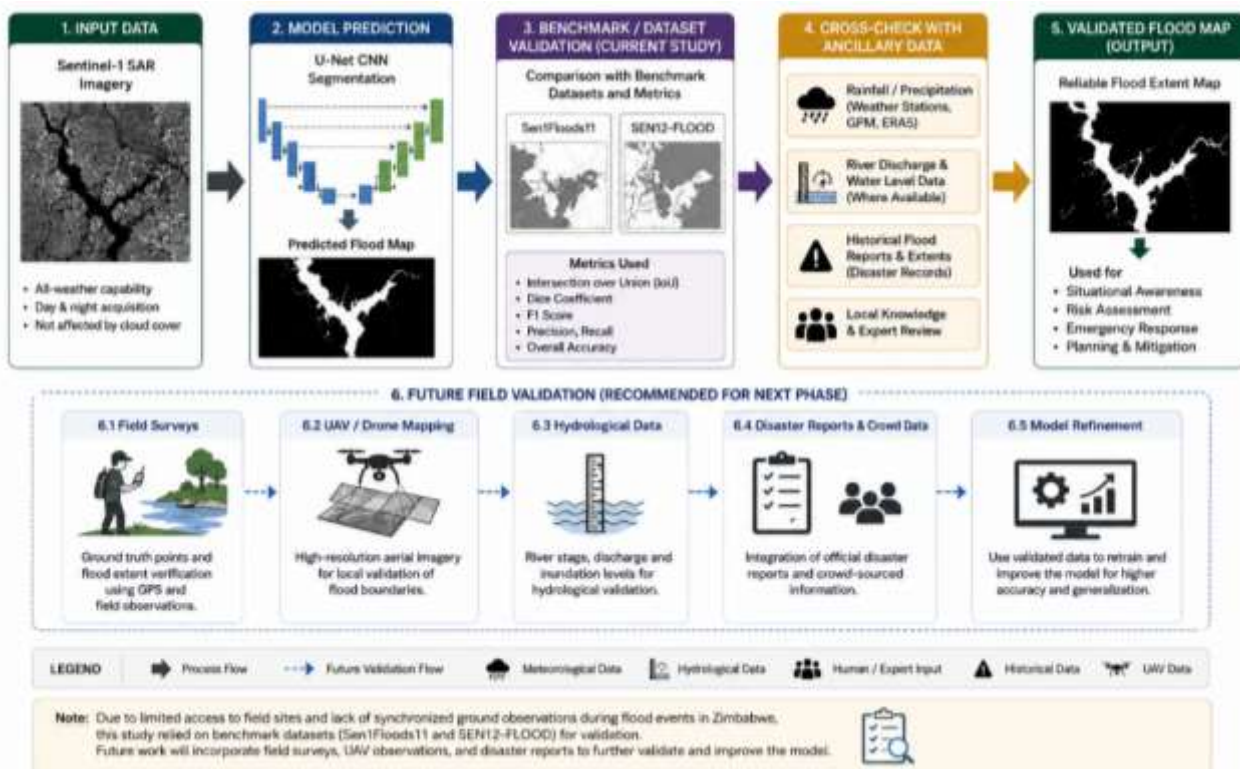


Figure 10: Validation framework adopted in the study showing benchmark dataset validation using Sen1Floods11 and SEN12-FLOOD, ancillary cross-checking with supporting data sources, and the proposed future field validation workflow for operational flood assessment.



CONCLUSION

This study presented a U-Net model for flood identification using Sentinel-1 radar imagery in Zimbabwe. The model achieved strong segmentation performance with high classification accuracy and overlap agreement metrics, demonstrating the applicability of SAR-based deep learning for flood monitoring in data-limited environments.

Future endeavors will concentrate on the integration of multimodal deep learning, the growth of region-specific SAR datasets, and the development of real-time flood forecasting systems to enhance predictive flood monitoring and early warning capabilities.

ADDITIONAL MATERIAL

Dataset availability

Sentinel-1 SAR imagery used in this study was obtained from the European Space Agency Copernicus Open Access Hub. Benchmark flood masks were derived from the Sen1Floods11 and SEN12-FLOOD datasets.

Code Availability

The implementation code, preprocessing scripts, and model training configurations used in this study are available through a public GitHub repository.

REFERENCES

1. Amit, S. N. K. B., & Aoki, Y. (2017). Disaster detection from aerial imagery with convolutional neural network. Proceedings - International Electronics Symposium on Knowledge Creation and Intelligent Computing, IES-KCIC 2017, 2017-January. <https://doi.org/10.1109/KCIC.2017.8228593>
2. Chanza, N., Siyongwana, P. Q., Williams-Bruinders, L., Gundu-Jakarasi, V., Mudavanhu, C., Sithole, V. B., & Manyani, A. (2020). Closing the Gaps in Disaster Management and Response: Drawing on Local Experiences with Cyclone Idai in Chimanimani, Zimbabwe. *International Journal of Disaster Risk Science*, 11(5). <https://doi.org/10.1007/s13753-020-00290-x>
3. Das, A., Abrar Rajin, S. M., Kah Ong Michael, G., Biswas, S., Billah, N., & Khan, R. (2025). Dual-Attention ResUNet With Masked Focal-Tversky Loss for Robust SAR-Based Flood Mapping. *IEEE Access*, 13, 201460–201477. <https://doi.org/10.1109/ACCESS.2025.3637023>
4. Dube, E., Mtapuri, O., & Matunhu, J. (2018). *Jamba-Journal of Disaster Risk Studies*. <https://doi.org/10.4102/jamba>
5. Edwing, D., Meng, L., Lv, S., & Yan, X. H. (2025). Characterizing Storm-Induced Coastal Flooding Using SAR Imagery and Deep Learning. *IEEE Journal of Selected Topics in Applied Earth Observations and Remote Sensing*, 18, 5619–5632. <https://doi.org/10.1109/JSTARS.2025.3530255>
6. Homepage, J., Hidayat, M. A., Latifah Husni, N., & Damsi, F. (2022). Image Processing Based Flood Detector Using Convolutional Neural Network (CNN) Within Surveillance Camera Pendeteksi Banjir dengan Image Processing Berbasis Convolutional Neural Network (. MALCOM: Indonesian Journal of Machine Learning and Computer Science, 2(October).
7. Huang, B., Li, P., Lu, H., Yin, J., Li, Z., & Wang, H. (2024). WaterDetectionNet: A New Deep Learning Method for Flood Mapping With SAR Image Convolutional Neural Network. *IEEE Journal of Selected Topics in Applied Earth Observations and Remote Sensing*, 17, 14471–14485. <https://doi.org/10.1109/JSTARS.2024.3440995>
8. Miau, S., & Hung, W. H. (2020a). River flooding forecasting and anomaly detection based on deep learning. *IEEE Access*, 8. <https://doi.org/10.1109/ACCESS.2020.3034875>
9. Miau, S., & Hung, W. H. (2020b). River flooding forecasting and anomaly detection based on deep learning. *IEEE Access*, 8, 198384–198402. <https://doi.org/10.1109/ACCESS.2020.3034875>



10. Moghimi, A., Welzel, M., Celik, T., & Schlurmann, T. (2024). A Comparative Performance Analysis of Popular Deep Learning Models and Segment Anything Model (SAM) for River Water Segmentation in Close-Range Remote Sensing Imagery. *IEEE Access*, 12, 52067–52085. <https://doi.org/10.1109/ACCESS.2024.3385425>
11. Munawar, H. S., Ullah, F., Qayyum, S., Khan, S. I., & Mojtahedi, M. (2021). Uavs in disaster management: Application of integrated aerial imagery and convolutional neural network for flood detection. *Sustainability (Switzerland)*, 13(14). <https://doi.org/10.3390/su13147547>
12. Munsaka, E., Mudavanhu, C., Sakala, L., Manjeru, P., & Matsvange, D. (2021). When Disaster Risk Management Systems Fail: The Case of Cyclone Idai in Chimanimani District, Zimbabwe. *International Journal of Disaster Risk Science*, 12(5). <https://doi.org/10.1007/s13753-021-00370-6>
13. Ntajal, J., Lamptey, B. L., Mahamadou, I. B., & Nyarko, B. K. (2017). Flood disaster risk mapping in the Lower Mono River Basin in Togo, West Africa. *International Journal of Disaster Risk Reduction*, 23. <https://doi.org/10.1016/j.ijdrr.2017.03.015>
14. Pally, R. J., & Samadi, S. (2022). Application of image processing and convolutional neural networks for flood image classification and semantic segmentation. *Environmental Modelling and Software*, 148. <https://doi.org/10.1016/j.envsoft.2021.105285>
15. Pascaline, W., House, R., McClean, D., & Below, R. (2018). UNISDR and CRED report: Economic Losses, Poverty & Disasters (1998 - 2017). *Unisdr - Cred*, 6.
16. Pech-May, F., Aquino-Santos, R., Alvarez-Cardenas, O., Arandia, J. L., & Rios-Toledo, G. (2024). Segmentation and Visualization of Flooded Areas Through Sentinel-1 Images and U-Net. *IEEE Journal of Selected Topics in Applied Earth Observations and Remote Sensing*, 17, 8996–9008. <https://doi.org/10.1109/JSTARS.2024.3387452>
17. Raspini, F., Bianchini, S., Ciampalini, A., Del Soldato, M., Solari, L., Novali, F., Del Conte, S., Rucci, A., Ferretti, A., & Casagli, N. (2018). Continuous, semi-automatic monitoring of ground deformation using Sentinel-1 satellites. *Scientific Reports*, 8(1). <https://doi.org/10.1038/s41598-018-25369-w>
18. Rathupetsane, E. M., & Kganyago, M. (2026). Geospatial analysis of flooding events using Sentinel-1 and Sentinel-2 data: a tale of two South African cities. *Environmental Monitoring and Assessment*, 198(5). <https://doi.org/10.1007/s10661-026-15321-1>
19. Ray, S., Goronga, T., Chigiya, P. T., & Madzimbamuto, F. D. (2022). Climate change, disaster management and primary health care in Zimbabwe. *African Journal of Primary Health Care and Family Medicine*, 14(1). <https://doi.org/10.4102/PHCFM.V14I1.3684>
20. Sharma, S. K., Misra, S. K., & Singh, J. B. (2020). The role of GIS-enabled mobile applications in disaster management: A case analysis of cyclone Gaja in India. *International Journal of Information Management*, 51. <https://doi.org/10.1016/j.ijinfomgt.2019.10.015>
21. Stateczny, A., Praveena, H. D., Krishnappa, R. H., Chythanya, K. R., & Babysarojam, B. B. (2023). Optimized Deep Learning Model for Flood Detection Using Satellite Images. *Remote Sensing*, 15(20). <https://doi.org/10.3390/rs15205037>
22. Thapa, A., Horanont, T., & Neupane, B. (2022). Parcel-Level Flood and Drought Detection for Insurance Using Sentinel-2A, Sentinel-1 SAR GRD and Mobile Images. *Remote Sensing*, 14(23). <https://doi.org/10.3390/rs14236095>
23. Umar, N., & Gray, A. (2023). Flooding in Nigeria: a review of its occurrence and impacts and approaches to modelling flood data. *International Journal of Environmental Studies*, 80(3). <https://doi.org/10.1080/00207233.2022.2081471>
24. Williamson, C., McCordic, C., & Doberstein, B. (2023). The compounding impacts of Cyclone Idai and their implications for urban inequality. *International Journal of Disaster Risk Reduction*, 86. <https://doi.org/10.1016/j.ijdrr.2023.103526>
25. Windheuser, L., Karanjit, R., Pally, R., Samadi, S., & Hubig, N. C. (2023). An End-To-End Flood Stage Prediction System Using Deep Neural Networks. *Earth and Space Science*, 10(1). <https://doi.org/10.1029/2022EA002385>
26. Wu, C., Yang, X., & Wang, J. (2019). Flood Detection in Sar Images Based on Multi-Depth Flood Detection Convolutional Neural Network. 2019 6th Asia-Pacific Conference on Synthetic Aperture Radar, APSAR 2019. <https://doi.org/10.1109/APSAR46974.2019.9048485>



27. Zhao, J., Li, Y., Matgen, P., Pelich, R., Hostache, R., Wagner, W., & Chini, M. (2022). Urban-Aware U-Net for Large-Scale Urban Flood Mapping Using Multitemporal Sentinel-1 Intensity and Interferometric Coherence. *IEEE Transactions on Geoscience and Remote Sensing*, 60. <https://doi.org/10.1109/TGRS.2022.3199036>